Impact-induced transition from damage to perforation

Attia Batool [ORCID], Gergő Pál, and Ferenc Kun [ORCID][*]

Department of Theoretical Physics, Doctoral School of Physics, Faculty of Science and Technology,
University of Debrecen, P.O. Box 400, H-4002 Debrecen, Hungary
and Institute for Nuclear Research, Hungarian Academy of Sciences (Atomki), P.O. Box 51, H-4001 Debrecen, Hungary

We investigate the impact-induced damage and fracture of a bar-shaped specimen of heterogeneous materials focusing on how the system approaches perforation as the impact energy is gradually increased. A simple model is constructed which represents the bar as two rigid blocks coupled by a breakable interface with disordered local strength. The bar is clamped at the two ends, and the fracture process is initiated by an impactor hitting the bar in the middle. Our calculations revealed that depending on the imparted energy, the system has two phases: at low impact energies the bar suffers damage but keeps its integrity, while at sufficiently high energies, complete perforation occurs. We demonstrate that the transition from damage to perforation occurs analogous to continuous phase transitions. Approaching the critical point from below, the intact fraction of the interface goes to zero, while the deformation rate of the bar diverges according to power laws as function of the distance from the critical energy. As the degree of disorder increases, farther from the transition point the critical exponents agree with their zero disorder counterparts; however, close to the critical point a crossover occurs to a higher exponent.

I. INTRODUCTION

Under a slowly increasing mechanical load materials typically undergo damaging and suffer ultimate failure at a critical load. The degree of materials' disorder has been found to play an essential role in the evolution of the fracture process [1–3]: at high disorder cracks nucleate already at relatively low load levels resulting in a gradual accumulation of damage as the load increases so that global failure occurs as the culmination of damaging. This stable cracking is accompanied by the emission of crackling noise [4], which proved to have a scale-free statistics with a high robustness against materials' details [5–9]. The evolution of the fracture process has also been found to obey time-to-failure power laws when approaching failure addressing the possibility of forecasting the imminent catastrophic event [10–13]. In the opposite limit of low disorder, ultimate failure is preceded by only a small amount of damage, an unstable crack emerges which gives rise to an abrupt failure [3].

Experimental and theoretical studies have revealed that fracture of disordered materials shows interesting analogies to phase transitions and critical phenomena [3,14,15]. In particular, loaded solids can be considered to be in a metastable state [16] so that the point of failure has been interpreted as a nucleation process in a first-order phase transition near a spinodal [14,17,18]. Other studies suggested that the transition from damage to fracture of highly disordered materials is analogous to continuous phase transitions due to the universal scaling laws emerging in the system near the critical point [19–23]. Recently, it has been clarified that tuning the amount of materials' disorder a transition occurs from brittle to quasibrittle behaviors, which proved to be continuous for long-range stress redistribution [24–29].

Studies of the phase transition nature of fracture phenomena have mostly been focused on uniaxial quasistatic loading conditions. However, both the time evolution and the final outcome of fracture processes also depend on how the load is applied on the specimen. For instance, in the usual Charpy impact test of dynamic fracture [30–33], the specimen is clamped at the ends and a hammer attached to the arm of a pendulum hits it in the middle resulting in a dynamic three point bending. Under such boundary and loading conditions, the damage localizes to a relatively thin layer of the specimen giving rise to a single growing crack. Depending on the energy of the hit, either the crack can terminate and the specimen suffers only partial failure, or it runs to the opposite boundary breaking the specimen into two pieces. This impact-induced transition from damage to complete perforation is driven by the interplay of materials disorder and the inhomogeneous stress field emerging due to the bending loading. In the present paper we study this transition as the energy of impact is varied. Based on a simple stochastic interface model of bending-induced breaking of bar-shaped specimens, we demonstrate that the transition is analogous to continuous phase transitions. Approaching the critical energy of perforation the fraction of the intact cross section goes to zero, while the deformation rate diverges according to power laws as a function of the distance from the critical point. We show that the critical exponents exhibit a crossover when the degree of disorder is varied; however, the transition remains continuous even in the limit of zero disorder.

———————
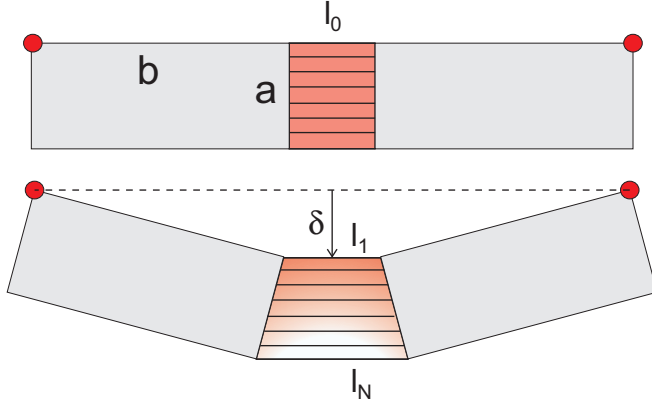[*]Corresponding author: ferenc.kun@science.unideb.hu

FIG. 1. Model of the specimen under three-point bending. The specimen is composed of two rigid blocks of extensions a and b coupled by an elastic interface. The interface is discretized in terms of breakable fibers with stochastic strength. The deformation of the bar due to impact is characterized by the deflection δ of its middle point. The impact loading results in a linear deformation profile along the interface, where the top and bottom fibers have the smallest l_1 and largest l_N length, respectively.

II. STOCHASTIC INTERFACE MODEL

To investigate the damage-perforation transition in impact loading processes, we use a simple model of the three-point bending setup of bar-shaped specimens. In the model the specimen is represented by two rigid blocks of side length a and b, which are glued together with a thin deformable interface of width $l_0 \ll b$. Clamping of the ends of the specimen is ensured by fixing the upper outer corners of the blocks around which they can perform rigid rotation. External loading is exerted by an impactor which hits the bar in the middle with a velocity pointing downward as illustrated in Fig. 1. As a consequence, the bar gets deflected in such a way that the entire deformation is accommodated by the elastic interface between the blocks. In order to capture fracturing of the bar, the interface is discretized by means of a bundle of parallel fibers of number N and length l_0, placed equidistantly between the blocks. The fibers do not have a bending rigidity, hence, they suffer only stretching when the bar is deflected. Fibers are assumed to have a linearly elastic behavior up to a threshold deformation ε_c^i, $i = 1, \ldots, N$ where they break irreversibly. Disorder of the material is represented such that individual fibers are characterized by an identical Young modulus Y; however, their breaking threshold is a random variable sampled from a probability density function $p(\varepsilon_c)$.

Due to the rigidity of the blocks the deformation of the specimen can be represented by a single variable δ, which is the deflection of the middle point of the bar. For illustration of the geometrical setup and the loading condition see Fig. 1. At a finite value of $\delta > 0$ the interface fibers suffer elongation Δl, which increases from top to bottom resulting in the opening of the interface. Based on the geometrical setup of Fig. 1, the actual length of fibers l_i can be expressed as

$$l_i = l_1 + 2\delta \frac{a}{b} \frac{i-1}{N-1}, \quad i = 1, \ldots, N, \tag{1}$$

where index i identifies the position of fibers starting from the top of the interface. The length of the first fiber l_1 reads as $l_1 = l_0 + 2(b - \sqrt{b^2 - \delta^2})$. Finally, the local elongation $\Delta l_i = l_i - l_0$ of fibers can be cast into the form

$$\Delta l_i = 2b - 2\sqrt{b^2 - \delta^2} + 2\delta \frac{a}{b} \frac{i-1}{N-1}, \tag{2}$$

which yields a linear deformation profile $\varepsilon_i = \Delta l_i / l_0$ along the interface.

Fracture is initiated by a collision with a body of mass m which hits the bar in the middle with an initial velocity v_0. For simplicity, we assume that the mass of the specimen is negligible compared to the impactor; furthermore, the impactor and the bar stay in contact during the entire fracture process. Hence, the initial kinetic energy $E_0 = 1/2mv_0^2$ imparted to the system will be partly transformed into the elastic energy E_{el} of the elongated fibers, and it gets partly dissipated, E_{dis}, by the breaking fibers. The energy balance of the collision process can be written in the form

$$E_0 = E_k(\delta(t)) + E_{el}(\delta(t)) + E_{\mathrm{dis}}(\delta(t)), \tag{3}$$

at any time t as the system evolves. On the right-hand side of Eq. (3) the first term E_k denotes the kinetic energy of the impactor

$$E_k = \tfrac{1}{2}mv^2 \tag{4}$$

moving at velocity v, which can be expressed as the derivative of the deflection $v = d\delta/dt$ of the specimen.

As the deflection increases fibers gradually get deformed and eventually break when exceeding their local breaking threshold. The elastic energy e_{el} stored by a single fiber of elongation Δl can be obtained as $e_{el} = (\frac{ac}{2Nl_0})Y\Delta l^2$, where the cross-sectional area ac/N is assigned to the fiber with $c = 1$ being the unit thickness of the sample. Hence, the energy E_{el} stored in the deformation of the entire bundle at deflection δ can be expressed analytically in terms of the disorder distribution of fibers as

$$E_{el}(\delta) = \frac{ac}{2Nl_0}Y\sum_{i=1}^{N}[1 - P(\varepsilon_i(\delta))]\Delta l_i(\delta)^2. \tag{5}$$

Here $P(x)$ represents the cumulative distribution of breaking thresholds so that the term $[1 - P(\varepsilon_i(\delta))]$ is the probability that the fiber at location i along the interface remained intact at the deflection δ. The energy E_{dis} dissipated by the broken fibers can be obtained as

$$E_{\mathrm{dis}} = \frac{ac}{2Nl_0}Y\sum_{i=1}^{N}\int_0^{\Delta l_i(\delta)} p(x)x^2\, dx, \tag{6}$$

assuming that the elastic energy stored in a fiber at the instant of its breaking is consumed to create the corresponding crack surface.

In order to study the effect of the degree of materials' disorder on the damage-perforation transition, for the breaking thresholds we introduce a uniform distribution of the form

$$p(\varepsilon_c) = 1/(2W) \quad \text{for} \quad \varepsilon_c^0 - W \leqslant \varepsilon_c \leqslant \varepsilon_c^0 + W. \tag{7}$$

The distribution $p(\varepsilon_c)$ is centered on ε_c^0, which denotes the average strength of fibers. The value of ε_c^0 is fixed in all the
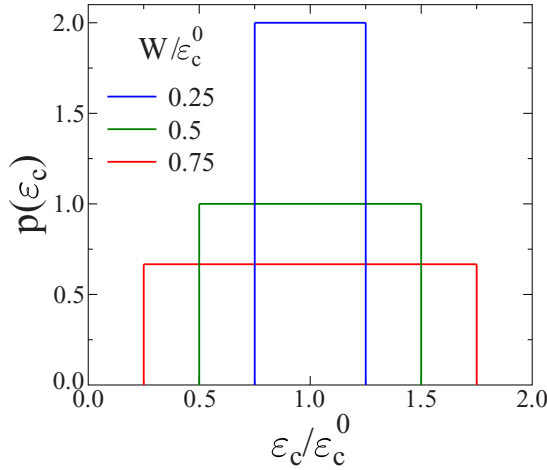
FIG. 2. Probability distribution $p(\varepsilon_c)$ of the breaking thresholds for three different values of the width $W/\varepsilon_c^0 = 0.25, 0.5, 0.75$. The average strength of fibers ε_c^0 is fixed; however, the degree of disorder can be tuned by varying the width W of the distribution. The value of W increases from top to bottom.

calculations; however, the degree of disorder of the system can be controlled by varying the width of the distribution W in the range $0 \leqslant W \leqslant \varepsilon_c^0$. The disorder distribution $p(\varepsilon_c)$ is illustrated in Fig. 2 for several values of W.

As the bar gets deflected during the impact process, a linear deformation profile builds up along the interface according to Eq. (2). In the absence of disorder $W = 0$ all breaking thresholds are the same, $\varepsilon_c^i = \varepsilon_c^0$ $(i = 1, \ldots, N)$, so that the fiber at the bottom of the interface $(i = N)$ breaks first. As a consequence, a crack starts and advances upwards until the last fiber $(i = 1)$ breaks. However, in the presence of disorder $W > 0$, the local strength ε_c^i and strain ε_i together determine the order of breaking so that the breaking sequence of fibers becomes random along the interface. Inverting Eq. (2) we can determine the deflection values δ_c^i where the individual fibers break,

$$\delta_c^i = \delta(i, \varepsilon_c^i), \quad i = 1, \ldots, N. \tag{8}$$

Note that the deflection thresholds δ_c^i depend on both the position i and strength ε_c^i of the fiber, which are independent variables. As the bar gets gradually deflected, fibers break in the increasing order of their deflection thresholds δ_c^i, $(i = 1, \ldots, N)$ resulting in a random sequence of breaking events along the interface in the linear deformation profile.

Computer simulation of the impact process is performed in the following way: in the initial state random threshold values ε_c^i $(i = 1, \ldots, N)$ are assigned to each fiber from the distribution (7). The deflection thresholds δ_c^i are determined from Eq. (8), which are then sorted into ascending order. The dissipated E_{dis} and elastic E_{el} energies are then calculated from the discrete form of Eqs. (5) and (6) as a function of δ. To analyze the damage-perforation transition, and to quantify the role of disorder, numerical calculations were performed varying the number of fibers in a broad range $N = 10^3$–10^7 at several values of the disorder parameter $W/\varepsilon_c^0 \in [0, 1]$. The geometrical layout of the specimen was fixed to $a = 1$, $b/a = 2.5$, and $l_0/a = 0.02$.
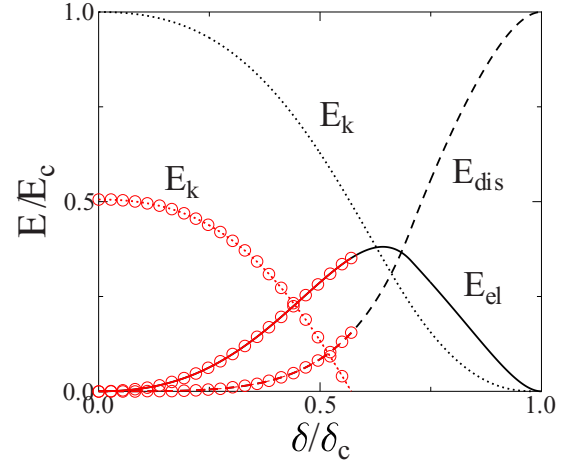

FIG. 3. The evolution of the energies during an impact process at the critical impact energy $E_0 = E_c$ as the function of deflection δ (black lines). In the final state E_c is completely dissipated by fiber breaking, hence, $E_{el}(\delta_c) = 0$ and $E_{\text{dis}}(\delta_c) = E_c$. Simulations were performed for an interface of $N = 10^6$ fibers with $W = \varepsilon_c^0$ for the threshold distribution (7). The red symbols highlight the case of a subcritical impact at $E_0 \approx E_c/2$.

III. ENERGETICS OF THE LOADING PROCESS

When the impactor hits the bar with an initial kinetic energy E_0, the bar gets deflected and the interface fibers start to break. If the input energy is low, the damage process stops at a maximum deflection δ_m where the interface suffers only a partial breaking keeping the integrity of the sample. When the maximum deflection δ_m is reached, the impactor stops; hence, the sum of the elastic and dissipated energies must be equal to the initial energy E_0 of impact

$$E_0 = E_{el}(\delta_m) + E_{\text{dis}}(\delta_m). \tag{9}$$

Inserting Eqs. (5) and (6) into Eq. (9) we can determine the initial impact energy E_0 needed to achieve a maximum deflection δ_m. When E_0 is sufficiently high, the damage process does not stop, and all fibers break so that the specimen gets perforated. This first occurs at the critical impact energy E_c, where deflection stops right at the breaking of the last fiber, with the largest critical deflection δ_c^i, defining the critical deflection δ_c of the system. It follows that the critical energy E_c is equal to the total dissipated energy $E_{\text{dis}}(\delta_c)$ needed to break through the entire interface.

The evolution of the energies stored in deformation $E_{el}(\delta)$ and dissipated by fiber breaking $E_{\text{dis}}(\delta)$ and the remaining kinetic energy $E_k(\delta)$ of the impactor are illustrated in Fig. 3 as a function of the deflection δ of the specimen at the critical energy $E_0 = E_c$ for a system containing N^6 fibers at the highest disorder $W/\varepsilon_0^c = 1$. The remaining kinetic energy of the impactor $E_k(\delta)$ was obtained as

$$E_k(\delta) = E_0 - [E_{el}(\delta) + E_{\text{dis}}(\delta)], \tag{10}$$

where the impact energy E_0 is determined from Eq. (9) at $\delta_m = \delta_c$ Since the disorder distribution in the example extends down to zero strength values, breaking starts already at a very small deflection. It can be observed in Fig. 3 that the dissipated energy E_{dis} monotonically increases, while the elastic energy
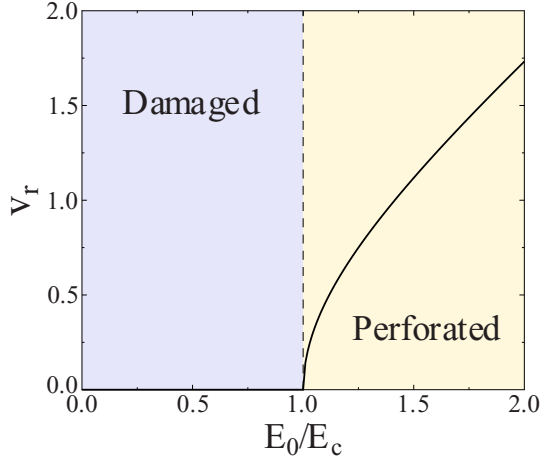
FIG. 4. The remaining velocity v_r of the impactor as a function of the imparted energy E_0. In the damage phase the impactor stops $v_r = 0$ at a partial failure of the specimen, while beyond the perforation limit $E_0 > E_c$ it keeps moving after the specimen broke into two pieces. The impactor is assumed to have a unit mass.

FIG. 5. The critical energy E_c of perforation as a function of the amount of disorder W/ε_0^c. The continuous line represents the analytical solution Eq. (12), while the symbols stand for numerical measurements. E_c is divided by the critical energy of the zero disorder case.

E_{el} has a maximum at a well-defined deflection value. The remaining kinetic energy E_k monotonically decreases reaching zero at the critical deflection. The figure also highlights the energetics of a subcritical impact $E_0 \approx E_c/2$ where the bar suffers damage in the form of fiber breaking but does not perforate. Since the elastic and dissipated energies are fully determined by the deflection of the bar δ, these curves coincide with their counterparts obtained at the critical input energy $E_0 = E_c$. However, at the maximum deflection δ_m, indicated by the end of the red curves, the kinetic energy is zero since the impactor stops.

In the supercritical phase $E_0/E_c > 1$ the specimen perforates, and hence, the impactor does not stop. The curves of the elastic and dissipated energies still coincide with the ones obtained at the critical point $E_0/E_c = 1$; however, the kinetic energy does not decrease to zero. Instead, the impactor continues moving with the remaining energy E_k attained at the critical deflection δ_c. This supercritical regime is illustrated by the so-called ballistic diagram of the system in Fig. 4 where the remaining velocity v_r of the impactor is plotted as a function of the input energy. The value of v_r was determined as

$$v_r = \sqrt{\frac{2}{m}(E_0 - E_c)}, \quad \text{for} \quad E_0 \geqslant E_c. \quad (11)$$

The two phases of the impact process are also highlighted in Fig. 4: in the damaged phase, below the critical impact energy, the impactor stops $v_r = 0$ at the maximum deflection δ_m reached, while the perforated phase is characterized by a finite value of the remaining velocity $v_r > 0$ since after breaking the bar the impactor retains a finite fraction of its initial energy.

IV. EFFECT OF DISORDER AND OF THE FINITE NUMBER OF FIBERS ON THE CRITICAL POINT

It is a crucial question how materials' disorder affects the impact-induced fracture of specimens. Based on the disorder
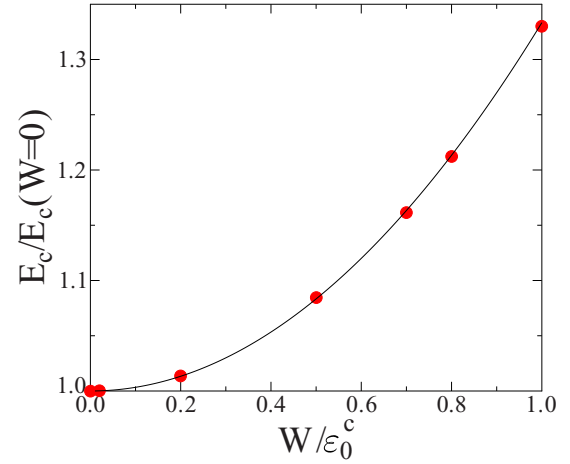
distribution (7) and on the expression of the dissipated energy (6) the critical energy E_c can be easily obtained. Since the energy dissipated by the breaking of a single fiber depends only on its breaking threshold ε_c but not on the corresponding deflection δ_c, the integral of Eq. (6) simplifies to integration over the range of the ε_c values. Hence, the disorder dependence of the critical energy E_c can be cast into the form

$$E_c = \frac{ac}{12Wl_0}\left[\left(\varepsilon_0^c + W\right)^3 - \left(\varepsilon_0^c - W\right)^3\right]. \quad (12)$$

It follows that E_c monotonically increases from $E_c(W = 0) = (ac/2l_0)(\varepsilon_c^0)^2$ at zero disorder to $E_c(W = \varepsilon_0^0) = (2ac/3l_0)(\varepsilon_c^0)^2$ at the highest one. It can be observed in Fig. 5 that the results of numerical measurements agree very well with the analytical expression (12) of the critical energy.

Since the critical energy E_c is an integrated quantity of the entire sample, it has only very low fluctuations when calculated from single samples using a finite number N of fibers to discretize the interface. However, the deflection values where the damaging starts δ_d and perforation occurs δ_c do have a strong dependence both on the number of fibers N and on the degree of disorder W. In order to quantify these effects, we performed computer simulations of the impact process varying N over four orders of magnitudes at several values of W. For a single sample the damage threshold δ_d and the critical deflection δ_c were identified as the deflection values where the first and last fiber breaking occur, respectively. Then these values were averaged over 1000 samples at each parameter set.

It can be observed in Figs. 6(a) and 6(b) that both the damage threshold δ_d and the critical deflection δ_c depend on the number of fibers N used to discretize the interface. However, δ_d decreases, while δ_c increases converging to well-defined asymptotic values $\delta_d(\infty, W)$ and $\delta_c(\infty, W)$ in the $N \to \infty$
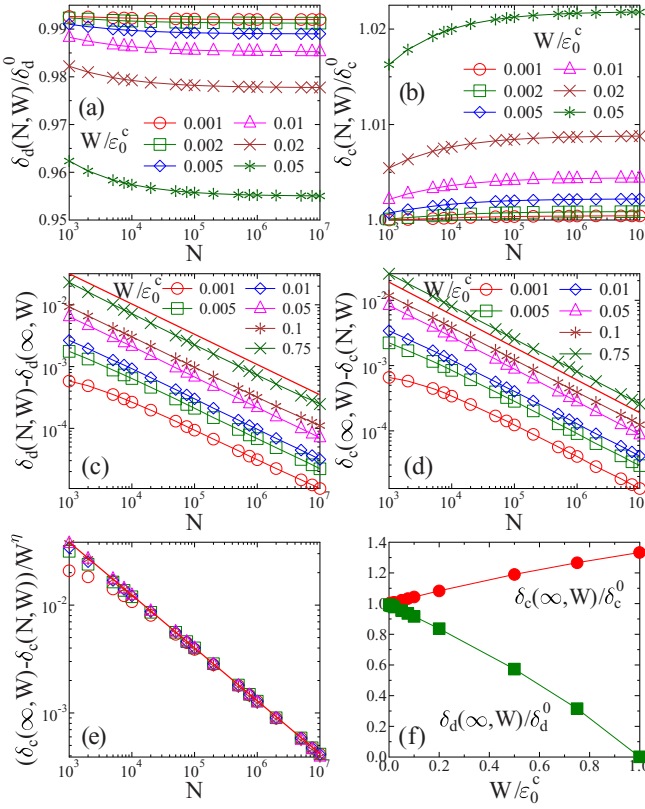
FIG. 6. The effect of the number of fibers N and the degree of disorder W on the damage threshold δ_d and on the critical deflection δ_c of the system. The damage threshold $\delta_d(N, W)$ (a) and the critical deflection $\delta_c(N, W)$ (b) are presented as function of N for several values of W. Both quantities converge to asymptotic values $\delta_d(\infty, W)$ and $\delta_c(\infty, W)$ in the limit $N \to \infty$. The deviation from the asymptotic value has a universal power-law dependence on the number of fibers in (c) and (d). The bold straight lines represent power laws of exponent $-1/2$. Rescaling the deviations by an appropriate power of W, the curves obtained at different disorders can be collapsed on top of each other. This scaling is demonstrated for $\delta_c(N, W)$ in (e). The asymptotic values of the damage threshold and critical deflection as a function of W are shown in (f).

limit. Note that both quantities are normalized by their zero disorder counterparts

$$\delta_d^0 = a\left[\sqrt{1 + \frac{bl_0\varepsilon_c^0}{a^2}} - 1\right], \tag{13}$$

$$\delta_c^0 = \frac{l_0\varepsilon_c^0}{2}\sqrt{\frac{4b}{l_0\varepsilon_c^0} - 1}, \tag{14}$$

which do not depend on N. It can be seen that increasing the amount of disorder W, the asymptotic values $\delta_d(\infty, W)$ and $\delta_c(\infty, W)$ more and more deviate from the zero disorder values. Figures 6(c) and 6(d) demonstrate that the convergence of the damage threshold $\delta_d(N, W)$ and of the critical deflection $\delta_c(N, W)$ to the corresponding asymptotic values shows interesting universal features; i.e., at any value of $W > 0$ the distances $\delta_d(N, W) - \delta_d(\infty, W)$ and $\delta_c(\infty, W) - \delta_c(N, W)$ tend to zero as a universal power law of the number of fibers N. The bold straight lines in the figures represent power laws

of exponent $-1/2$. The value of the exponent does not depend on the degree of disorder; however, the curves get shifted with respect to each other for increasing W. Figure 6(e) shows that rescaling the critical deflections δ_c with an appropriate power η of the degree of disorder W, the curves obtained at different W values can be collapsed on the top of each other. (The same systematics holds also for the damage threshold δ_d, not shown in the figure.) Based on the above numerical analysis we can cast the N and W dependence of the damage threshold and of the critical deflection into the following scaling forms:

$$\delta_d(N, W) = \delta_d(\infty, W) + AW^\eta N^{-\mu}, \tag{15}$$

$$\delta_c(N, W) = \delta_c(\infty, W) - BW^\eta N^{-\mu}, \tag{16}$$

where the scaling exponents have the values $\eta = 1/2$ and $\mu = 1/2$.

Equations (15) and (16) highlight that the asymptotic values of the damage and perforation thresholds both depend on the degree of disorder W. We determined $\delta_d(\infty, W)$ and $\delta_c(\infty, W)$ in such a way that they were finely tuned to obtain the best straight lines in Figs. 6(c) and 6(d) on a double logarithmic plot. The final outcome is presented in Fig. 6(f), where both the asymptotic damage threshold and critical deflection are normalized by their zero disorder counterparts given by Eqs. (13) and (14). It can be observed that for growing disorder the damaging of the interface starts earlier, while perforation is reached at a higher deflection if a sufficient amount of energy is exerted to the system. An important outcome of the analysis is that for a sufficiently fine discretization the results do not depend on the number of fibers.

In the following study of the perforation transition the number of fibers of the discretization was fixed to $N = 10^6$.

V. APPROACH TO THE CRITICAL POINT

In order to understand how the system approaches the critical point of perforation, numerical calculations were performed varying the input energy E_0 below E_c at several values of the degree of disorder W. Figure 7 presents the maximum deflection δ_m reached during the impact process as a function of the imparted energy E_0. It can be observed that δ_m monotonically increases with E_0 up to the critical deformation $\delta_c = \delta_m$ attained at $E_0 = E_c$. However, the deflection rate $\delta_m' = d\delta_m/dE_0$ is not monotonous; i.e., it can be inferred from the curves that starting from a relatively high value δ_m' first decreases at low energies reaching a finite minimum which is then followed by a growing deformation rate and seems to diverge as the critical energy is approached. Note that although the critical energy E_c is an increasing function of the degree of disorder W (see Fig. 5); i.e., higher energy is needed to break the sample, at the same fraction E_0/E_c of E_c the maximum deflection δ_m takes a larger value for higher W.

Gradually increasing the energy of impact, the increasing final state deformation is accompanied by a growing damage of the interface. To characterize the damage state of the bar we determined the fraction of intact fibers $n = N_i/N$, where N_i denotes the number of surviving fibers when the maximum deflection is reached at E_0. Figure 8 illustrates that n is a monotonically decreasing function of the imparted energy E_0 starting from one and converging to zero as the critical point of
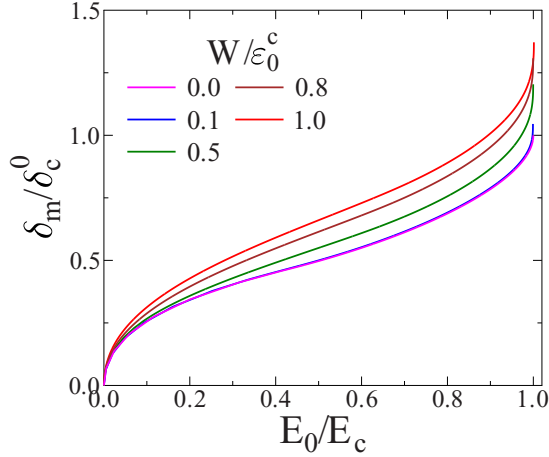
FIG. 7. Maximal deflection δ_m of the bar reached as a function of the impact energy E_0 for several disorder strengths W. The value of δ_m is nondimensionalized by division with the critical deflection δ_c^0 of the zero disorder case. The value of W increases from bottom to top.

perforation E_c is approached. Note that at lower disorder the $n(E)$ curves start with a constant regime $n = 1$, since the final state deflection has to surpass the damage threshold $\delta_m > \delta_d$ to initiate the breaking of fibers. The figure also demonstrates that at a given fraction of the critical energy E_0/E_c the surviving load bearing cross section n of the sample gets lower, implying a higher damage $d = 1 - n$ when the disorder is higher.

In order to understand the nature of the transition from partial failure to perforation, we analyzed in detail how the system behaves in the vicinity of the critical point E_c. It has been shown above that as the input energy increases, the critical point of perforation is approached through an acceleration of the deformation of the bar in such a way that δ'_m diverges in the limit $E_0 \to E_c$. It means that close to E_c the system becomes more and more susceptible to the gradual increase of the impact energy responding with a rapidly growing deflec-
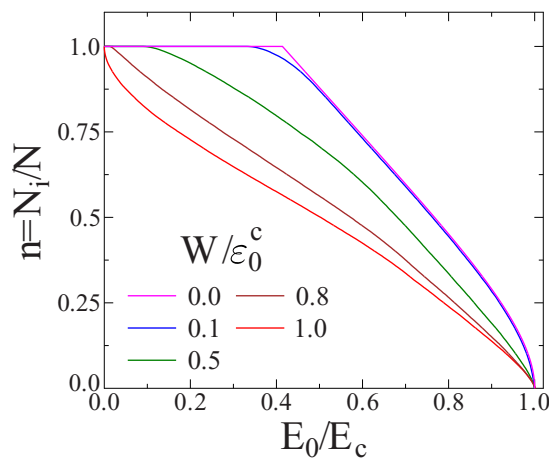

FIG. 8. Fraction of intact fibers $n = N_i/N$ as a function of the impact energy E_0 for several values of the degree of disorder W. The value of W increases from right to left.
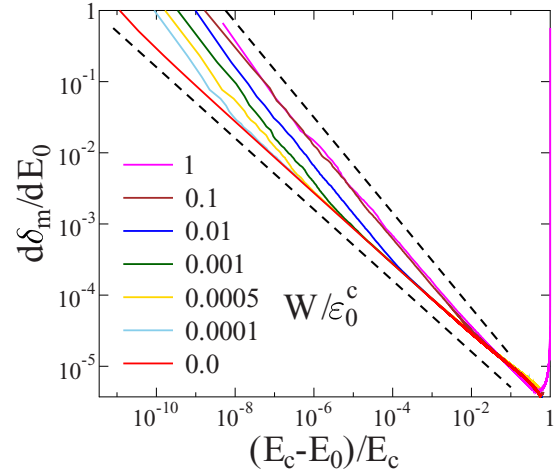

FIG. 9. Derivative of the maximal deflection δ_m with respect to the impact energy E_0 as a function of the relative distance from the critical point $(E_c - E_0)/E_c$ for several values of the degree of disorder W. The dashed lines represent power laws of exponent $1/2$ and $2/3$. As the disorder W increases the crossover point between the two power-law regimes shifts to the right. The value of W increases from left to right.

tion. For a quantitative characterization of this susceptibility, we determined the deflection rate δ'_m by numerical differentiation of the $\delta_m(E_0)$ curves for several disorder strengths W. Figure 9 demonstrates that for zero disorder $W = 0$ the deflection rate diverges as a power law of the distance from the critical point

$$\delta'_m \sim (E_c - E_0)^{-\gamma}, \qquad (17)$$

where the exponent γ has the value $\gamma = 1/2$. Note that the quality of the power-law approximation is excellent; for a system of $N = 10^6$ fibers a straight line is obtained on a double logarithmic plot over eight orders of magnitude. It is important to emphasize that at finite disorder $W > 0$ when the fibers have a stochastic variation of strength, the power-law divergence prevails; however, a crossover occurs between two regimes of different exponents: farther from E_c the value of the power-law exponent coincides with its zero disorder counterpart $\gamma = 1/2$; however, close to the critical point the deflection accelerates characterized by a higher exponent $\gamma = 2/3$.

The emergence of scaling in the vicinity of the critical point is further supported by the behavior of the fraction of intact fibers n. Figure 10 demonstrates that replotting n as a function of the distance from the critical point $E_c - E_0$ an excellent power law is obtained for the zero disorder case

$$n \sim (E_c - E_0)^\beta. \qquad (18)$$

The value of the exponent is $\beta = 1/2$. In the perforation phase $E_0 > E_c$ the fraction of intact fibers n is identically zero, while in the phase of partial failure it has a nonzero value $n > 0$ going to zero as a power law of the distance from the critical point when approaching E_c. Due to this behavior, n can be considered as the order parameter of the transition and β is the order parameter exponent. At finite disorder $W > 0$, the qualitative behavior of the curves is similar to the deflection
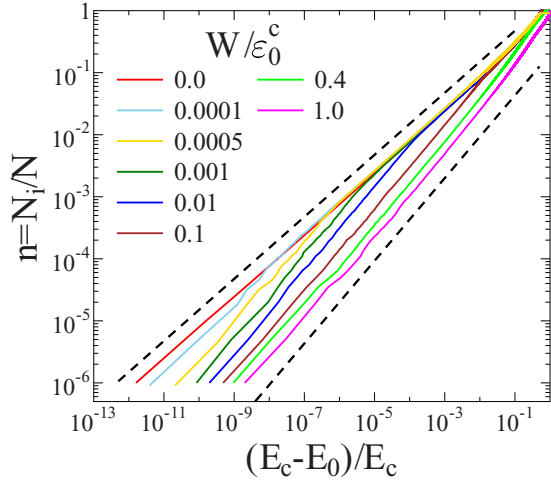
FIG. 10. The fraction of intact fibers as a function of the relative distance from the critical point $\Delta = (E_c - E_0)/E_c$ for several values of the degree of disorder W. The dashed lines represent power laws of exponent $1/2$ and $2/3$. The value of W increases from left to right.

rate, i.e., the power-law functional form prevails; however, a crossover occurs again between two different exponents. Close to failure n approaches zero with a higher exponent $\beta = 2/3$; however, farther from the critical point the exponent takes its zero disorder value $\beta = 1/2$ (see Fig. 10).

Comparing Figs. 9 and 10 it can be observed that the position of the crossover point Δ^* depends on the degree of disorder: As the disorder increases the crossover where the exponents γ and β switch to their higher value occurs earlier at larger distances from the critical point. Using the data of the deflection rate in Fig. 9 we determined the value of the crossover point Δ^* as the position of intersection of two fitted straight lines of exponents $1/2$ and $2/3$ in a double logarithmic representation. The results are presented in Fig. 11, where Δ^* is plotted as a function of W. It can be observed that approaching the limit of zero disorder Δ^* goes
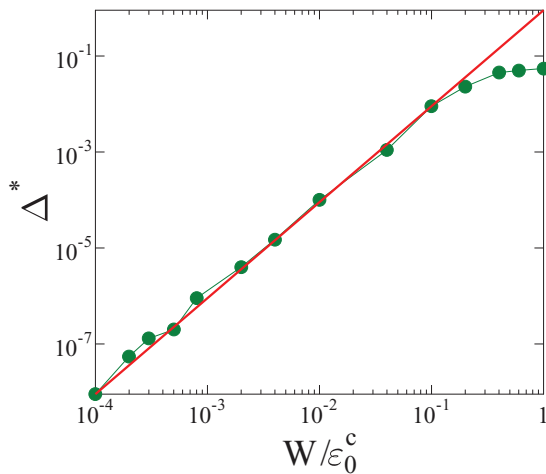

FIG. 11. The value of the crossover point Δ^* as a function of the degree of disorder W/ε_0^c. The straight line represents a power law of exponent 2.0.

to zero since the entire curves of n and δ_m' are characterized by a single exponent of value $1/2$. Increasing the degree of disorder W, the value of Δ^* rapidly grows and levels off above $W/\varepsilon_0^c \approx 0.15$. The figure also demonstrates that along the increasing regime the curve of $\Delta^*(W)$ can be very well approximated by a power law

$$\Delta^* \sim W^\xi, \qquad (19)$$

where the exponent is $\xi = 2.0 \pm 0.05$. The saturation of the crossover point Δ^* implies that beyond a certain value of W further increasing the amount of disorder does not have a relevant effect. To understand the emergence of this behavior, the spatial structure of damaging has to be analyzed. At zero disorder perforation occurs such that a crack starts at the bottom of the interface and proceeds upwards as the impactor moves forward. On the contrary, in the presence of disorder $W > 0$, fibers break in a spatially random sequence along the interface. Due to the interplay of the strain gradient (2) and the disorder (7), a complex damage profile emerges along the interface: at a given deflection δ highly deformed fibers at the bottom of the interface are broken with a higher probability forming a crack, while the ones on the top have a high chance to be intact. The two regimes are separated by a sparse sequence of broken and intact fibers which behaves as a process zone ahead of the crack tip. As the degree of disorder W is increased the process zone gets wider, and for sufficiently large values of W it can span the entire interface. This situation of strong disorder occurs if at the deformation where the top of the interface may get damaged, $\varepsilon_1(\delta) > \varepsilon_0^c - W$, the bottom of the interface may still be intact, $\varepsilon_N(\delta) < \varepsilon_0^c + W$. Here ε_1 and ε_N are the strains of the fibers at the top and bottom of the bar, respectively. Making use of Eqs. (2) and (7) and assuming that $b \gg \varepsilon_0^c + W$ the condition for strong disorder can be cast into the form

$$W^* \approx \frac{a^2}{2b}\left[\sqrt{1 + \frac{4b\varepsilon_0^c}{a^2}} - 1\right]. \qquad (20)$$

It follows that for $W > W^*$ the disorder is so high that no crack is formed, and damage can occur anywhere along the interface although it is more probable to break fibers closer to the bottom. The results imply that the relevance of disorder in the damaging of the interface is determined together by the geometrical layout of the sample a, b, by the average strength of fibers ε_0^c, and by the width of the strength distribution W. The crossover point Δ^* depends on W only in the regime of weak disorder $W < W^*$. The value of $W^* \approx 0.22$ obtained from Eq. (20) has a reasonable agreement with the numerical findings.

VI. DISCUSSION AND CONCLUSIONS

We investigated the impact-induced fracture of a bar-shaped specimen with the aim to understand how perforation occurs as the impact energy is gradually increased. In the modeling approach the bar is represented as two rigid blocks glued together with an elastic interface which can undergo damaging as the bar deforms. The interface is discretized in terms of a bundle of parallel fibers which allows for a simple representation of materials' disorder by the random strength of fibers. We implemented the loading condition commonly

used in the Charpy impact test to determine the fracture toughness of materials; i.e., a dynamically induced three-point bending test is considered.

Our analytical and numerical calculations showed that depending on the imparted energy E_0, the outcome of the impact process can be classified into two states: at low values of the impact energy the bar suffers only a finite deflection accompanied by damage, resulting in a partial failure of the specimen. However, exceeding a critical energy value E_c the impact results in global failure breaking the specimen into two pieces. The transition between the damaged and perforated phases occurs at a well-defined critical energy.

In order to characterize how the transition occurs as the impact energy is gradually increased, we studied the behavior of the deflection rate and of the surviving cross section when approaching the perforation critical point. Numerical analysis revealed that the deflection rate diverges, while the fraction of surviving fibers goes to zero as power laws of the distance from the critical point analogous to continuous phase transitions. The power-law behavior holds for any degree of disorder with universal exponents; however, at finite disorders a crossover occurs between two power-law regimes of different exponents: farther from the critical point the critical exponents coincide with their zero disorder counterparts, but in the vicinity of the critical point both quantities are characterized by a higher exponent. The crossover point proved to have a power-law dependence on the degree of disorder in the range of weak disorder, while it remains nearly constant for strongly disordered samples.

The effect of the degree of disorder on the nature of the transition from damage to complete breakdown has been studied in various types of systems [15,23,25,29,34–36]. These investigations have revealed that below a certain degree of disorder fracture becomes abrupt, so that to obtain power-law scaling the amount of disorder has to exceed a threshold value. On the contrary, it is a unique feature of our system that even in the limit of zero disorder the damage-perforation transition occurs analogous to continuous phase transitions characterized by critical power laws. The reason for this important difference is the loading condition. Our impact loading is assumed to be applied under three-point bending conditions so that the stress and strain of fibers are inhomogeneous increasing linearly with distance from the impact site. Additionally, the advancing impactor gives rise to a loading which is essentially strain controlled; i.e., the position of the impactor determines the load but in such a way that fiber breakings gradually release the load on the specimen. The strain gradient in the specimen and the releasing effect of

breaking fibers together stabilize the damage process even in the case of zero disorder. For the phase transition nature of the damage-perforation transition the global response of the system, ensured by the two rigid blocks of the bar, plays an essential role. The main simplification of the model is that it does not capture the stress concentration arising at the tip of the propagating crack in real materials. However, the model calculations imply that the damage-perforation phase transition should occur also in the presence of stress enhancements due to the overall bending of the bar.

It can be seen from Eq. (2) that the magnitude of the strain gradient is controlled by the geometrical layout of the sample; i.e., the gradient is proportional to the ratio a/b of the side lengths of the bar. Hence, in the limit of $a/b \to 0$, for very long and thin bars all fibers have nearly the same load. It can be seen from Eq. (20) that in this limit the value of W^* separating weak and strong disorders tends to zero so that the disorder-driven crossover disappears, and the system is always in the strong disorder phase.

In our detailed study we considered uniformly distributed breaking thresholds varying the degree of disorder through the width of the distribution. Other members of the universality class of thin-tailed distributions, decreasing rapidly away from the average, like the Weibull and Gaussian distributions, are expected to give rise qualitatively to the same fracture processes [37]. In particular, we repeated the calculations with the Weibull distribution varying the Weibull exponent, while the scale parameter of the distribution was fixed, and obtained the same results as in the uniform case. However, power-law distributed disorder results in a higher degree of complexity. Due to the fat tail of the threshold distribution the crossover from weak to strong disorder may disappear in spite of the strain gradient. Work in this direction is in progress.

[1] H. J. Herrmann and S. Roux (ed.), *Statistical Models for the Fracture of Disordered Media*, Random materials and processes (North-Holland, Amsterdam, 1990).

[2] M. Alava, P. K. Nukala, and S. Zapperi, Adv. Phys. **55**, 349 (2006).

[3] S. Biswas, P. Ray, and B. K. Chakrabarti, *Statistical Physics of Fracture, Beakdown, and Earthquake: Effects of Disorder and Heterogeneity*, Statistical Physics of Frac-

ture and Breakdown (John Wiley & Sons, New York, 2015).

[4] J. Rosti, X. Illa, J. Koivisto, and M. J. Alava, J. Phys. D **42**, 214013 (2009).

[5] A. Garcimartin, A. Guarino, L. Bellon, and S. Ciliberto, Phys. Rev. Lett. **79**, 3202 (1997).

[6] S. Santucci, L. Vanel, and S. Ciliberto, Phys. Rev. Lett. **93**, 095505 (2004).

[7] M. B. J. Meinders and T. van Vliet, Phys. Rev. E **77**, 036116 (2008).

[8] S. Deschanel, L. Vanel, N. Godin, and S. Ciliberto, J. Stat. Mech.: Theor. Exp. (2009) P01018.

[9] E. K. Salje and K. A. Dahmen, Annu. Rev. Condens. Matter Phys. **5**, 233 (2014).

[10] D. Sornette, Proc. Natl. Acad. Sci. U.S.A. **99**, 2522 (2002).

[11] G. F. Nataf, P. O. Castillo-Villa, P. Sellappan, W. M. Kriven, E. Vives, A. Planes, and E. K. H. Salje, J. Phys.: Condens. Matter **26**, 275401 (2014).

[12] X. Jiang, H. Liu, I. G. Main, and E. K. H. Salje, Phys. Rev. E **96**, 023004 (2017).

[13] V. Kádár, G. Pál, and F. Kun, Sci. Rep. **10**, 2508 (2020).

[14] S. Zapperi, P. Ray, H. E. Stanley, and A. Vespignani, Phys. Rev. Lett. **78**, 1408 (1997).

[15] S. Roy, S. Biswas, and P. Ray, Phys. Rev. E **96**, 063003 (2017).

[16] A. Buchel and J. P. Sethna, Phys. Rev. Lett. **77**, 1520 (1996).

[17] S. Zapperi, P. Ray, H. E. Stanley, and A. Vespignani, Physica A **270**, 57 (1999).

[18] F. Kun and H. J. Herrmann, J. Mat. Sci. **35**, 4685 (2000).

[19] D. Sornette and J. Andersen, Eur. Phys. J. B **1**, 353 (1998).

[20] Y. Moreno, J. B. Gomez, and A. F. Pacheco, Phys. Rev. Lett. **85**, 2865 (2000).

[21] G. Caldarelli, F. D. Di Tolla, and A. Petri, Phys. Rev. Lett. **77**, 2503 (1996).

[22] D. Bonamy, S. Santucci, and L. Ponson, Phys. Rev. Lett. **101**, 045501 (2008).

[23] C. Roy and S. S. Manna, Phys. Rev. E **100**, 012107 (2019).

[24] C. B. Picallo, J. M. López, S. Zapperi, and M. J. Alava, Phys. Rev. Lett. **105**, 155502 (2010).

[25] E. Karpas and F. Kun, Europhys. Lett. **95**, 16004 (2011).

[26] Z. Danku and F. Kun, J. Stat. Mech.: Theor. Exp. (2016) 073211.

[27] C. Roy, S. Kundu, and S. S. Manna, Phys. Rev. E **91**, 032103 (2015).

[28] O. Ramos, P.-P. Cortet, S. Ciliberto, and L. Vanel, Phys. Rev. Lett. **110**, 165506 (2013).

[29] S. Roy and P. Ray, Europhys. Lett. **112**, 26004 (2015).

[30] T. A. Siewert and M. P. Manahan, *Pendulum Impact Testing: A Century of Progress* (ASTM International, Baltimore, MD, 2000).

[31] D. Francois and A. Pineau, *From Charpy to Present Impact Testing* (Elsevier, Amsterdam, 2002).

[32] F. Kun, G. B. Lenkey, N. Takács, and D. L. Beke, Phys. Rev. Lett. **93**, 227204 (2004).

[33] Z. Danku, G. B. Lenkey, and F. Kun, Appl. Phys. Lett. **106**, 064102 (2015).

[34] J. V. Andersen, D. Sornette, and K. Leung, Phys. Rev. Lett. **78**, 2140 (1997).

[35] D. Bonamy and E. Bouchaud, Phys. Rep. **498**, 1 (2011).

[36] U. S. Kachhwah and S. Mahesh, Phys. Rev. E **101**, 063002 (2020).

[37] A. Hansen, P. Hemmer, and S. Pradhan, *The Fiber Bundle Model: Modeling Failure in Materials*, Statistical Physics of Fracture and Breakdown (Wiley, New York, 2015).